JACS
JOURNAL OF THE AMERICAN CHEMICAL SOCIETY

ARTICLE

pubs.acs.org/JACS

Evidence for Concerted Electron Proton Transfer in Charge Recombination between $FADH^-$ and $^{306}Trp^\bullet$ in *Escherichia coli* Photolyase

Agnieszka A. Zieba,[†] Caroline Richardson,[‡] Carlos Lucero,[†] Senghane D. Dieng,[†] Yvonne M. Gindt,[‡] and Johannes P. M. Schelvis*[,†]

[†]Department of Chemistry and Biochemistry, Montclair State University, 1 Normal Avenue, Montclair, New Jersey 07043, United States

[‡]Department of Chemistry, Lafayette College, Hugel Science Center, Easton, Pennsylvania 18042, United States

ABSTRACT: Proton-coupled electron-transfer (PCET) is a mechanism of great importance in protein electron transfer and enzyme catalysis, and the involvement of aromatic amino acids in this process is of much interest. The DNA repair enzyme photolyase provides a natural system that allows for the study of PCET using a neutral radical tryptophan ($Trp^\bullet$). In *Escherichia coli* photolyase, photoreduction of the flavin adenine dinucleotide (FAD) cofactor in its neutral radical semiquinone form ($FADH^\bullet$) results in the formation of $FADH^-$ and $^{306}Trp^\bullet$. Charge recombination between these two intermediates requires the uptake of a proton by $^{306}Trp^\bullet$. The rate constant of charge recombination has been measured as a function of temperature in the pH range from 5.5 to 10.0, and the data are analyzed with both classical Marcus and semi-classical Hopfield electron transfer theory. The reorganization energy associated with the charge recombination process shows a pH dependence ranging from 2.3 eV at pH ≤ 7 and 1.2 eV at pH(D) 10.0. These findings indicate that at least two mechanisms are involved in the charge recombination reaction. Global analysis of the data supports the hypothesis that PCET during charge recombination can follow two different mechanisms with an apparent switch around pH 6.5. At lower pH, concerted electron proton transfer (CEPT) is the favorable mechanism with a reorganization energy of 2.1−2.3 eV. At higher pH, a sequential mechanism becomes dominant with rate-limiting electron-transfer followed by proton uptake which has a reorganization energy of 1.0−1.3 eV. The observed 'inverse' deuterium isotope effect at pH < 8 can be explained by a solvent isotope effect that affects the free energy change of the reaction and masks the normal, mass-related kinetic isotope effect that is expected for a CEPT mechanism. To the best of our knowledge, this is the first time that a switch in PCET mechanism has been observed in a protein.

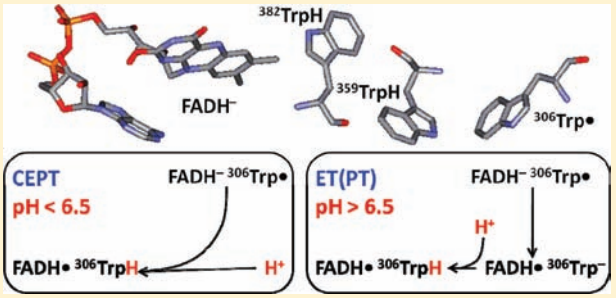

INTRODUCTION

Proton-coupled electron-transfer (PCET) plays an essential role in important physiological processes.[1,2] The simultaneous transfer of an electron and proton avoids the high energy intermediate states that would be involved with the separate transfer of each charged particle. In addition, by coupling electron transfer to proton transfer (or vice versa), rates of transfer and catalysis can be controlled to occur on a desired timescale. PCET has been observed and proposed to take place in many proteins and enzymes, and it has been examined extensively with model compounds and by theory.[1−10] PCET can follow different mechanisms and can be dissociative or associative, or occur as hydrogen atom transfer. In the most common schemes, PCET occurs following a sequential or concerted mechanism. In a sequential mechanism, electron transfer (ET) is followed by proton transfer (PT) or PT is followed by ET. In a concerted mechanism, the electron and proton are transferred simultaneously, and this process is referred to as concerted electron proton transfer (CEPT).

There is much interest for PCET in proteins that use amino acid radical intermediates along with modified proteins and peptides.[1,2,11−13] Recently, Hammarström and co-workers published a series of papers in which they studied PCET in Ru-tyrosine and Ru-tryptophan model compounds.[14−16] They demonstrated that PCET can switch from CEPT to sequential ET and PT in those model compounds as a function of pH. They also showed that one can discriminate between these two mechanisms by determining the reorganization energy from the temperature dependence of the rate constant by using the Marcus theory of electron transfer if the proton release is accounted for in the free-energy term by a pH-dependent entropy term.[15,16] In their model compound studies, CEPT is characterized by a large reorganization energy of 2.4 eV, a large change in free energy, a pH-dependent rate constant, and a significant kinetic isotope effect (KIE) in D_2O solutions.

In *Escherichia coli* photolyase, charge recombination following photoreduction of its neutral radical flavin adenine dinculeotide ($FADH^\bullet$) is strongly pH-dependent[17−19] and could involve PCET.

Received: January 6, 2011
Published: May 02, 2011

dx.doi.org/10.1021/ja2001488 | *J. Am. Chem. Soc.* 2011, 133, 7824–7836

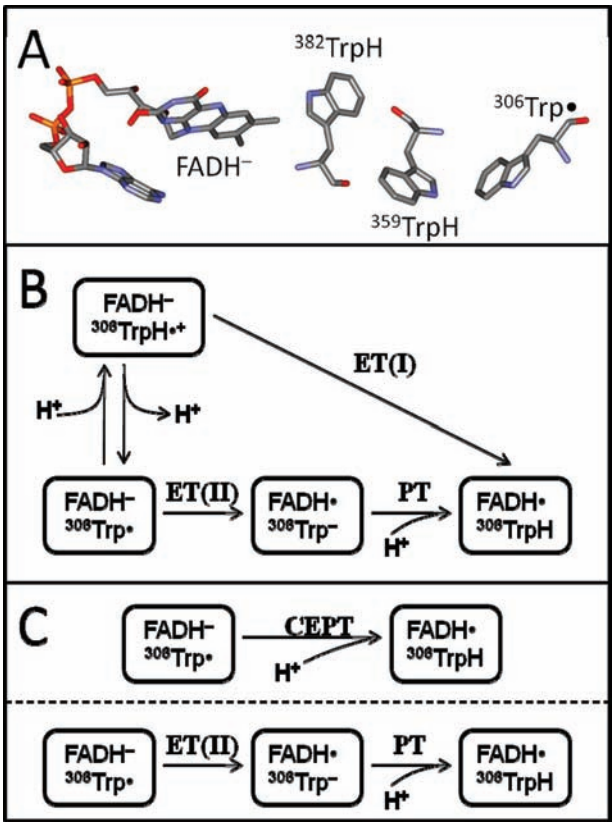

Figure 1. (A) Tryptophan triad in *E. coli* photolyase with charge-separated state $FADH^-$ and $^{306}Trp^{\bullet}$.[32] (B) ET-model for charge recombination proposed by Byrdin et al.[19] The equilibrium between $^{306}TrpH^{\bullet+}$ and $^{306}Trp^{\bullet}$ with a pK_a of 4 is proposed to modulate the charge recombination mechanism. $^{306}TrpH^{\bullet+}$ follows a pure electron transfer mechanism, ET(I), and $^{306}Trp^{\bullet}$ follows a pure, rate-limiting electron transfer mechanism, ET(II), which is followed by proton transfer (PT). (C) CEPT-model for charge recombination proposed on the basis of current work. The CEPT mechanism is dominant at lower pH values, and the ET(II) mechanism (pure, rate-limiting electron transfer followed by proton transfer) is favored at high pH values.

E. coli photolyase is a DNA repair enzyme that repairs cyclobutane pyrimidine dimers in DNA using a light-driven electron-transfer mechanism.[20] Besides the FAD cofactor as its redox active site, photolyase contains a 5,10-methenyltetrahydrofolate polyglutamate (MTHF), which can transfer excitation energy to the FAD cofactor but is not essential for enzyme function. The active form of the enzyme requires a fully reduced FAD as $FADH^-$.[21] The enzyme is isolated with the FAD cofactor in its neutral radical semiquinone form, $FADH^{\bullet}$, which can be photoreduced by a nearby tryptophan residue ($^{382}TrpH$) after absorption of a photon.[17,22−26] In this paper, we explicitly indicate the presence of the indole proton as TrpH or $TrpH^{\bullet+}$ in the reactions. $^{382}TrpH$ is part of a tryptophan triad that also includes $^{359}TrpH$ and $^{306}TrpH$ (see Figure 1A) and is conserved in all photolyases and cryptochromes.[27−30] Originally, it was proposed that the cationic radical formed on $^{382}TrpH$ ($^{382}TrpH^{\bullet+}$) moved along the triad to $^{359}TrpH$ and, finally, to $^{306}TrpH$ in less than 10 ns, but a newly proposed model favors a rapid formation of the $FADH^--^{306}TrpH^{\bullet+}$ charge separated pair in less than 50 ps with a quantum yield of about 19%.[17,30,31] With a time constant of less than 1 μs, $^{306}TrpH^{\bullet+}$ deprotonates to give the $FADH^-—^{306}Trp^{\bullet}$ charge separated pair.[17,21,32] The distance between the FAD-cofactor and $^{306}TrpH$ is about 15 Å, while the individual steps measure 3.5−5.5 Å.[33] Although the Trp-triad has been widely accepted as the photoreduction pathway, a competitive tunneling pathway through the α-helix that connects ^{306}Trp with ^{366}Phe has also been proposed.[26] In the absence of exogenous electron donors, charge recombination occurs on the millisecond timescale.[17−19,34] The charge recombination process is affected by the presence of substrate and is pH-dependent.[17−19] The latter observation suggests that a PCET mechanism may be at work. Although the charge recombination between $FADH^-$ and $^{306}Trp^{\bullet}$ involves the uptake of a proton, it has been recently described by a model with two pure electron-transfer mechanisms (Figure 1B).[19] The first mechanism which dominates at low pH is pure electron transfer from $FADH^-$ to $^{306}TrpH^{\bullet+}$, and the second mechanism which dominates at high pH is pure, rate-limiting electron transfer from $FADH^-$ to $^{306}Trp^{\bullet}$ followed by the uptake of a proton by $^{306}Trp^-$. It was proposed that the pH-dependence in the charge recombination mechanism originates from the fast equilibrium between $^{306}TrpH^{\bullet+}/^{306}Trp^{\bullet}$ with a pK_a of 4. A CEPT mechanism was not considered due to the lack of a significant deuterium isotope effect. An 'inverted' deuterium isotope effect was observed below pH 8.

In this work, we test the model for charge recombination between $FADH^-$ and $^{306}TrpH^{\bullet+}/^{306}Trp^{\bullet}$ that was postulated by Byrdin et al.[19] We have measured the temperature dependence of the rate constant of charge recombination in the pH range from 5.5 to 10. We have determined that the reorganization energy of charge recombination is pH-dependent and ranges from 2.1 to 2.3 eV at pH 5.5 and from 1.3 to 1.5 eV at pH 10. The pH-dependence suggests that two mechanisms are at work, and the high reorganization energy at lower pH is indicative of a CEPT mechanism. Global analysis of our data shows that the charge recombination process is best described by CEPT below pH 7 and by rate-limiting ET followed by PT above pH 7. The transition point between the two mechanisms lies around pH 6.5. Although a pH-dependent switch in PCET mechanism has been observed for model compounds and proposed to occur for tyrosine (Y_D) radical reduction in photosystem II,[16,35] to the best of our knowledge, this is the first time that such a switch has been reported in a protein. The CEPT mechanism is characterized by an 'inverse' isotope effect, most likely explained by the solvent isotope effect, which favorably affects the thermodynamic parameters for electron transfer in D_2O solution and masks the real kinetic isotope effect.

MATERIALS AND METHODS

Materials. Chemicals were purchased from Sigma-Aldrich and Acros Organics and used without further purification. D_2O was from Cambridge Isotope Laboratories, Inc.

Sample Preparation. Photolyase was overexpressed, isolated, and purified as described elsewhere.[23,36] Purified photolyase was stored in 0.4 M K_2SO_4 and 20 mM potassium phosphate (pH 7.0) at −80 °C. Buffer exchange was done by two dilution and concentration cycles with the use of 30 kDa NMWL centrifugal filter devices (Amicon Ultra, Millipore). The following buffers, each with 0.4 M K_2SO_4, were prepared: 20 mM citric acid for pH 5.5 and 6.0, 20 mM potassium phosphate for pH 7.0 and 8.0, 20 mM sodium pyrophosphate for pH 9.0, and 75 mM sodium bicarbonate for pH 9.5 and 10.0. A typical sample had a volume of 250 μL with photolyase at a concentration of 80 μM. The concentration of the flavin neutral radical in photolyase was determined from the absorbance at 580 nm with an extinction coefficient of $\varepsilon_{580} = 4800\ M^{-1}\ cm^{-1}$.[37]

dx.doi.org/10.1021/ja2001488 |J. Am. Chem. Soc. 2011, 133, 7824–7836

The samples for experiments in D_2O solutions were prepared in the buffers described above. The pD of each solution was determined by adding 0.4 to pH electrode reading.[38,39]

Transient Absorption Measurements. Transient absorption spectroscopy was performed on a home-built system described below. A 5 ns pulse at 532 nm from a Surelite Nd:YAG laser (I-20, Continuum) was used to excite the sample with a pulse energy of 50−60 mJ at a 10 Hz repetition rate. The laser light was diffused through a mounted ground glass diffuser (220 GRIT, ThorLabs) to provide homogenous excitation of the sample. The probe light was generated with a 75 W Xe lamp (Optical Building Blocks) and focused onto the sample with a lens. Infrared and ultraviolet light were removed from the probe beam with a heat filter (FSR-KG3, Newport), and a 50 nm bandwidth of light was selected by using a 550 nm cut-on filter and a 600 nm cut-off filter (FGL550S and FES0600, ThorLabs). Shutters and controllers (SH05 and SC10, ThorLabs, and VS25S2ZM1 and VCM-DI, Uniblitz) were used to block the laser pulses and the probe light to avoid unnecessary exposure of the sample to light. The shutter controllers were regulated by a pulse generator (9514 Plus Series, Quantum Composers) which was triggered on the preceding laser pulse detected with a photodiode (210 DET, ThorLabs). The probe light and the laser pulse made a 90° angle at the center of a quartz cuvette that was placed in a TLC 50 temperature-controlled cuvette holder attached to the TC 125 temperature controller (Quantum North West) contained in a sample box (Model 2007, Optical Building Blocks). The cuvette holder was affixed to a circulating water bath (Little Giant Pump, Franklin Electric) and in-house dry air for cooling and purging purposes, respectively. The temperature was varied from −5 to +35 °C with 5 °C increments and monitored with a thermocouple (OMEGA) inside the sample. The transmitted probe light was focused into a monochromator (Model 2000, Optical Building Blocks), and the transmitted light intensity was detected with a photodiode (DET 36A, ThorLabs). The signal was attenuated with a variable terminator (VT1, Thorlabs) and recorded with a digital oscilloscope (TDS 2022, Tektronix). The output of the Xe lamp was directly monitored with a DET 210 photodiode connected to the oscilloscope through a variable attenuator to correct for fluctuations in the probe light.

At each temperature, two sets of 5−10 transient absorption traces were averaged. Three to five data sets were obtained for the temperature range at each pH. Samples were replaced upon the first signs of sample degradation (FAD oxidation) or trapping of FAD in its fully reduced state. Both cases led to loss of signal and poor signal-to-noise ratios. Neither oxidized nor fully reduced flavin contributed to the transient absorption signal under the excitation and detection conditions due to selective excitation of $FADH^•$ at 532 nm.[23] The repetition rate of the laser was varied between 10 and 2 Hz depending on the observed decay kinetics to ensure a full decay and stabilization of the signal between laser excitation pulses.

Spectroscopic Measurements of Fully Reduced and Semiquinone FAD. Fully reduced FAD in solution and in photolyase at various pH(D) values was prepared by purging samples with N_2(g) for 10 min. FAD in solution was photoreduced in the presence of 20 mM EDTA. $FADH^•$ in photolyase was photoreduced with visible light (λ > 420 nm) in the presence of 20 mM dithiothreitol, and the MTHF cofactor was removed by using UV-light (λ = 300−400 nm) for photodegradation.[34] All irradiation was done with filtered light from a 75 W Xe lamp for 10 min at 0 °C. The progress of the photoreduction and photodegradation processes was monitored by checking the UV−vis absorption spectrum.

The spectrum of the FAD semiquinone in photolyase was monitored as a function of pH(D) using UV−vis absorption and resonance Raman spectroscopy. The resonance Raman spectra were obtained with 532 nm excitation as described elsewhere.[40]

Determination of the $FADH^-/FADH^•$ Reduction Potential. The $FADH^-/FADH^•$ reduction potential in H_2O solutions as a function of pH was determined using a spectroelectrochemical method as described previously.[40,41] The reduction potential was also measured in a D_2O buffer solution at pD 7.0. The buffer solutions were prepared as described above. No correction was made to the Ag/AgCl reference electrode for the D_2O solvent.

Data Analysis. For each pH and temperature, the rate constant of the charge recombination process was determined by fitting the transient absorption traces to a monoexponential decay function. The quality of the fit was not improved when a biexponential decay function was used. The averaged charge recombination rate constants, k_{ET}, at each pH as a function of temperature, T, were fit to the Marcus equation for electron transfer to obtain the reorganization energy, λ, and the electronic coupling matrix element, H_{AB}:[42,43]

$$k_{ET} = \frac{2\pi}{\hbar}\frac{H_{AB}^2}{\sqrt{4\pi\lambda k_B T}}\exp\left(-\frac{(\Delta G^\circ + \lambda)^2}{4\lambda k_B T}\right) \quad (1)$$

where $\hbar$ is Planck's constant, k_B is Boltzmann's constant, and ΔG° is the change in standard free energy.

At room temperature, the energy $\hbar\omega$ that is associated with the characteristic frequency of the nuclear motion coupled to the electron transfer is larger than k_BT, and it is necessary to analyze the data also with a semi-classical expression that makes quantum corrections to the classical Marcus expression.[44,45] The semi-classical Hopfield expression for the rate constant of electron transfer is as follows:

$$k_{ET} = \frac{2\pi}{\hbar}H_{AB}^2[2\pi\lambda\hbar\omega\coth(\hbar\omega/2k_BT)]^{-1/2}\exp\left(-\frac{(\Delta G^\circ + \lambda)^2}{2\lambda\hbar\omega\coth(\hbar\omega/2k_BT)}\right) \quad (2)$$

For the analysis, three possible values for $\hbar\omega$ are used: 200, 70, and 25 meV. The change in standard free energy is given by:

$$\Delta G^\circ = e[E_m^0(FADH^-/FADH^•) - E_m^0(Trp^•/TrpH)] \quad (3)$$

where $E_m^0(FADH^-/FADH^•)$ and $E_m^0(Trp^•/TrpH)$ are the reduction potentials of the FAD cofactor and ^{306}TrpH in photolyase. $E_m^0(Trp^•/TrpH)$ is pH dependent due to the uptake of a proton during the charge recombination process.[46,47] This introduces a reaction entropy term, which is approximated by the mixing term associated with proton release in bulk water and is given by:

$$\Delta S_{reaction} \approx \Delta S_{uptake} \quad (4a)$$

$$\Delta S_{uptake} = -\Delta S_{mixing} = -R\ln(10)\text{pH} \quad (4b)$$

where R is the gas constant. Data on other contributions to the reaction entropy are currently not known for this reaction, but their total contribution is considered to be negligibly small following the analysis by Sjödin et al. for their model compounds.[16]

The introduction of the entropy term results in a new free energy change of reaction, $\Delta G^{\circ\prime}$, given by:

$$\Delta G^{\circ\prime} = \Delta G^\circ + (T - 295)\cdot\Delta S_{uptake} \quad (5)$$

The entropy correction at T = 295 K is set to zero because the contribution of the reaction entropy is included in the measurement of $E_m^0(Trp^•/TrpH)$ at that temperature.[47] Data analysis was done using Origin 7.0 (Originlab) and Igor Pro 4.07 (Wavemetrics).

RESULTS

Temperature and pH-Dependence of Charge Recombination in Photolyase. Photoreduction of $FADH^•$ results in the formation of $FADH^-$ and $^{306}Trp^•$ and corresponds to the disappearance of the $FADH^•$ absorbance between 450 and 650 nm.[17,24] The rate constant of charge recombination can be measured by

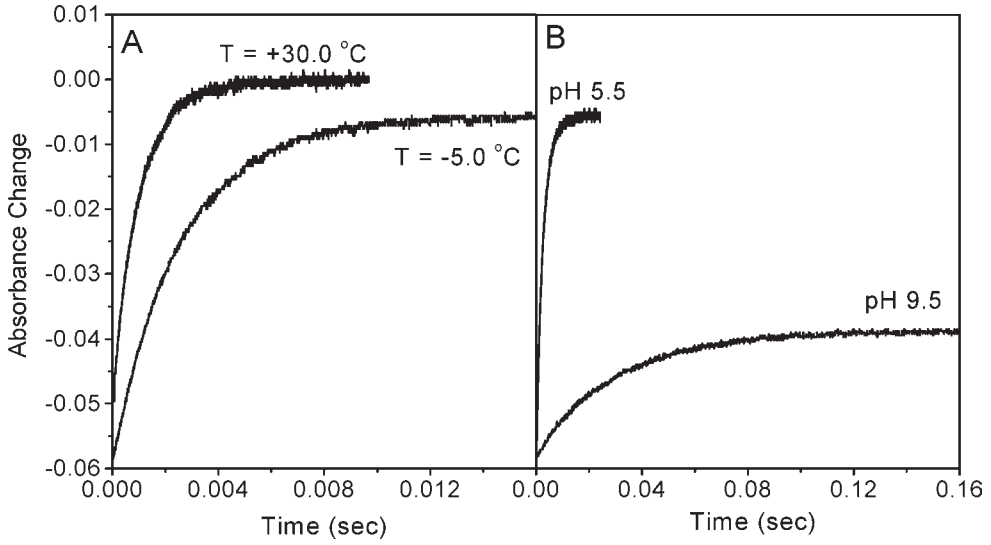

Figure 2. Temperature and pH dependence of charge recombination in photolyase monitored at 580 nm following excitation at 532 nm with a 5 ns pulse. (A) Photolyase at pH 5.5 and at 30.0 °C and at −5.0 °C. (B) Photolyase at −5.0 °C and at pH 5.5 and pH 9.5.

Table 1. Rate Constant (s^{-1}) of Charge Recombination in DNA Photolyase as a Function of Temperature and pH

T (K)	pH 5.5	pH 6.0	pH 7.0	pH 8.0	pH 9.0	pH 9.5	pH 10.0
268.15	330 (±70)	270 (±50)	52.1 (±1.0)	32.86 (±0.03)	32.1 (±0.6)	32.95 (±0.17)	33.0 (±0.7)
273.15	360 (±60)	260 (±90)	58.9 (±1.2)	37.1 (±0.7)	36.7 (±1.6)	36.7 (±0.3)	37.1 (±0.5)
278.15	400 (±70)	290 (±100)	68 (±5)	42.8 (±0.7)	42.0 (±1.6)	41.8 (±0.5)	42.0 (±1.5)
283.15	450 (±75)	320 (±110)	79 (±4)	48.9 (±0.4)	47.6 (±1.9)	47.7 (±0.7)	47.1 (±1.0)
288.15	520 (±90)	370 (±120)	93 (±8)	56.8 (±0.8)	53.9 (±0.3)	54.3 (±1.0)	54.3 (±0.9)
293.15	580 (±110)	450 (±180)	115 (±16)	64 (±4)	62.5 (±0.7)	67.2 (±1.0)	68 (±7)
298.15	720 (±140)	500 (±190)	133 (±16)	76.6 (±1.8)	73.6 (±0.5)		
303.15	870 (±150)	590 (±220)	160 (±20)	89 (±4)	88.9 (±1.7)		
308.15	1070 (±80)	750 (±370)	178 (±7)	109 (±14)			

monitoring the recovery of the $FADH^{\bullet}$ absorbance. It has been shown previously that the rate constant of charge recombination is independent of the probe wavelength.[17,18] Figure 2 shows the reappearance of the $FADH^{\bullet}$ absorbance at 580 nm due to the following charge recombination process:

$$FADH^{-} + {}^{306}Trp^{\bullet} + H^{+} \rightarrow FADH^{\bullet} + {}^{306}TrpH \qquad (6)$$

Although $Trp^{\bullet}$ also absorbs at 580 nm,[17,24] it disappears with the same kinetics that describe the reappearance of $FADH^{\bullet}$ and will not complicate the analysis of the transient absorption traces. The temperature dependence of the reaction at pH 5.5 (Figure 2A) shows absorption changes at −5 and 30 °C with time constants for the charge recombination reaction of 2.6 and 1.0 ms, respectively.

The pH-dependence of the charge recombination reaction is illustrated in Figure 2B. At −5 °C, the reaction occurs with a time constant of 3.0 ms at pH 5.5 and 30.3 ms at pH 10. This pH-dependence of the rate constant for charge recombination is in agreement with earlier measurements.[17−19] The averaged rate constants of the charge recombination reaction as a function of pH and temperature are listed in Table 1. The larger standard deviations of the rate constant at lower pH values are due to the strong pH-dependence of the reaction in that pH range. Despite differences in rate constants between data sets, the reorganization energy values that were obtained at low pH show only a small standard deviation between data sets (see below). Therefore, the uncertainty of the rate constants at lower pH values does not affect the interpretation of our data. At lower temperatures but mainly at higher pH values, the transient absorption change does not return completely to zero. Despite this complication, we determine the same rate constants as measured by others under these conditions.[19] At higher pH values, there may be a heterogeneity in the availability of proton donors that interferes with charge recombination, resulting in two populations, one that can undergo charge recombination and one that cannot, trapping the FAD cofactor in the $FADH^{-}$ state. The population that does not undergo charge recombination does not contribute to the observed rate constant and does not affect our analysis. This apparent incomplete charge recombination will be of interest for future studies and may elucidate the nature of the proton donor(s).

Determination of Reorganization Energy and Electronic Coupling Matrix Element. The reorganization energy can be determined experimentally by measuring either the temperature dependence or the free energy dependence of the electron transfer rate constant.[43] Since it is non-trivial to modify the cofactors in DNA photolyase, we have used the temperature dependence approach with the approximation that the reduction potentials of the species involved are constant over the temperature range used. Figure 3 shows the temperature dependence of the rate constant

of charge recombination at pH 7.0. The values of λ and H_{AB} were obtained with and without the entropy correction (eq 5) by fitting the temperature dependence of the rate constant with the classical Marcus theory of electron transfer (eq 1). The thermodynamic parameters that were used for the fitting procedure are listed in Table 2. The $E^0_m(FADH^-/FADH^\bullet)$ in *E. coli* photolyase was determined experimentally for the pH-range of 6−9 (data not shown) with no obvious pH dependence of $E^0_m(FADH^-/FADH^\bullet)$ observed (Table 2). The value of $E^0_m(Trp^\bullet/TrpH)$ (in mV) was determined by using an empirical formula:[46,47]

$$E^0_m(Trp^\bullet/TrpH) = 1070 - (pH - pK_a)\cdot 53 \qquad (7)$$

with $pK_a = 3.7$ for $TrpH^{\bullet+}$. We used the data from the study by Tommos et al. since that study involved TrpH in a protein and reflects our system more closely.[47]

For the data in Figure 3, values of $\lambda = 1.88$ eV and $H_{AB} = 7.1 \times 10^{-7}$ eV were obtained when the entropy correction was included; the results are listed in Table 3. The small standard deviations of λ shown in the table indicate a good reproducibility at each pH value. The inset in Figure 3 shows the variation of λ with pH when analyzed with or without the entropy correction. It is clear that the inclusion of the entropy correction affects the magnitude of the reorganization energy but not its pH-dependence. At pH 7.0, the average reorganization energy is 1.98 ± 0.09 eV with entropy correction and increases to 2.53 ± 0.10 eV when the entropy term is omitted.

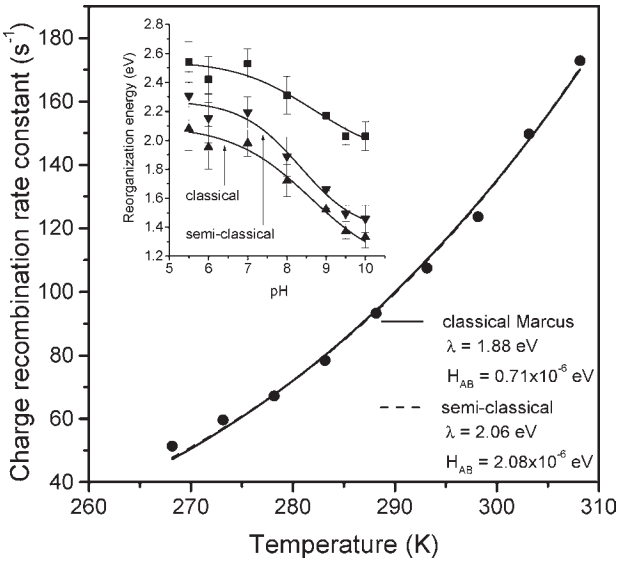

Figure 3. Temperature dependence of the rate constant of charge recombination in *E. coli* photolyase at pH 7.0 fitted to the classical Marcus (solid line) and semi-classical Hopfield (dashed line, $\hbar\omega$ = 25 meV) theory of electron transfer (eq 1 and eq 2) with correction for entropy (eq 5). Inset: The reorganization energy as a function of pH with (▲) and without (■) the entropy correction from classical Marcus theory and with entropy correction (▼) from semi-classical Hopfield ($\hbar\omega$ = 25 meV) theory. The solid lines are added to guide the eye.

Charge Recombination in D_2O Buffer Solutions. The kinetic isotope effect (KIE) on the charge recombination rate constant measured at 10 °C as a function of pH(D) is shown in Figure 4. Above pH(D) 8.0, a small isotope effect of 1.1−1.4 is observed, while an 'inverse' isotope effect is observed below pH(D) 8.0, in agreement with an earlier report (see inset Figure 4).[19] The values of the thermodynamic parameters in D_2O are needed to determine λ and H_{AB} for the charge recombination reaction in the D_2O.

We measured the $FADH^-/FADH^\bullet$ reduction potential in *E. coli* photolyase at pD 7.0 to be +45 (±6) mV versus NHE (data not shown), a small increase of 45 mV compared to the potential at pH 7.0. Since we found no significant pH-dependence of $E^0_m(FADH^-/FADH^\bullet)$, we also assumed that the reduction potential remained constant within the pD range of this study. A slightly more positive reduction potential is in agreement with other studies of FAD-containing proteins.[48,49] The entropy change associated with the proton uptake in D_2O solutions was assumed to have the same value as in H_2O solutions with pH replaced by pD (eq 4). Finally, the value of the $Trp^\bullet/TrpH$ reduction potential in D_2O solution is not available; however, it has been well-documented that weak acids experience an increase in pK_a in D_2O, represented by $\Delta pK_a = pK_a^D - pK_a^H$, in solution and proteins.[50−54] It has been proposed that the Trp cationic radical has $\Delta pK_a = 0.56$ in D_2O.[19] To estimate $E^0_m(Trp^\bullet/TrpD)$ in D_2O solutions, we modified eq 7 by shifting the pH-dependence by 0.56:

$$E^0_m(Trp^\bullet/TrpD) = 1070 - (pD - pK_a^D)\cdot 53 \qquad (8)$$

with $pK_a^D = 3.7 + \Delta pK_a = 4.26$ for $TrpD^{\bullet+}$ in D_2O solutions. All the thermodynamic parameters used to fit the experimental data are shown in Table 2, and the results for λ and H_{AB} with the thermodynamic parameters for the D_2O data are shown in Table 3. The dependence of λ on pD is shown in the inset of Figure 4. The value of λ obtained is always slightly smaller in D_2O experiments than in H_2O experiments. We want to emphasize that there is some uncertainty in the thermodynamic fit parameters for D_2O experiments which may give rise to this discrepancy. However, λ does show the same dependence on pD as on pH, and a significant increase in λ arises from removing

Table 2. Thermodynamic Parameters Used for Fits with Classical Marcus (eq 1) and Semi-Classical Hopfield (eq 2) Theory to the Temperature Dependence of the Charge Recombination Rate Constant

pH(D)	$E^0_m(FADH^-/FADH^\bullet)$ (mV)	$E^0_m(Trp^\bullet/TrpH)$ (mV)[a]	$\Delta G°$ (eV)	ΔS_{uptake} (10^{-3} eV/K)[b]
5.5	16[c] (45)[d]	975 (1004)	−0.951 (−0.959)	−1.09
6.0	24 ± 10 (45)[d]	948 (978)	−0.924 (−0.933)	−1.19
7.0	0 ± 6 (45 ± 6)	895 (925)	−0.895 (−0.880)	−1.39
8.0	11 ± 7 (45)[d]	842 (872)	−0.831 (−0.827)	−1.59
9.0	14 ± 4 (45)[d]	789 (819)	−0.775 (−0.774)	−1.79
9.5	8.5[c] (45)[d]	763 (792)	−0.754 (−0.747)	−1.89
10.0	7.5[c] (45)[d]	736 (766)	−0.728 (−0.721)	−1.98

[a] Data from ref 47 estimated with empirical formulas eq 7 and eq 8 for H_2O and D_2O, respectively. [b] ΔS_{uptake} is assumed the same in H_2O and D_2O solutions (see text). [c] Values extrapolated from measurements at pH 6.0 through pH 9.0. [d] Values for D_2O experiments in parentheses.

dx.doi.org/10.1021/ja2001488 |*J. Am. Chem. Soc.* 2011, 133, 7824–7836

Table 3. pH-Dependence of the Reorganization Energy (λ) and Electronic Coupling Matrix Element (H_{AB}) Obtained from a Fit with Classical Marcus (eq 1) and Semi-Classical Hopfield (eq 2) Theory to the Charge Recombination Rate Constants As a Function of Temperature in H_2O and D_2O Solutions

	classical without entropy correction		classical with entropy correction		semi-classical with entropy correction and $\hbar\omega$ = 25 meV	
pH	λ (eV)	H_{AB} (10^{-6} eV)	λ (eV)	H_{AB} (10^{-6} eV)	λ (eV)	H_{AB} (10^{-6} eV)
5.5	2.54 (±0.14)	21.5	2.08 (±0.15)	3.33	2.30 (±0.17)	11.3
6.0	2.42 (±0.16)	13.3	1.95 (±0.15)	2.00	2.15 (±0.17)	5.22
7.0	2.53 (±0.10)	11.5	1.98 (±0.09)	1.15	2.19 (±0.11)	3.75
8.0	2.31 (±0.13)	5.56	1.72 (±0.11)	0.40	1.89 (±0.14)	1.26
9.0	2.17 (±0.01)	3.64	1.52 (±0.01)	0.24	1.66 (±0.01)	0.64
9.5	2.03 (±0.06)	2.34	1.37 (±0.05)	0.16	1.49 (±0.06)	0.38
10.0	2.03 (±0.10)	2.91	1.33 (±0.07)	0.16	1.46 (±0.10)	0.40
pD	λ (eV)	H_{AB} (10^{-6} eV)	λ (eV)	H_{AB} (10^{-6} eV)	λ (eV)	H_{AB} (10^{-6} eV)
5.5	2.38 (±0.04)	20.0	1.97 (±0.03)	3.63	2.13 (±0.04)	9.52
6.0	2.37 (±0.02)	10.0	1.92 (±0.02)	2.12	2.08 (±0.03)	5.87
7.0	2.41 (±0.02)	8.45	1.88 (±0.02)	0.93	2.05 (±0.02)	2.65
8.0	2.25 (±0.01)	3.41	1.67 (±0.01)	0.31	1.80 (±0.01)	0.80
9.0	2.02 (±0.05)	1.52	1.41 (±0.04)	0.13	1.51 (±0.04)	0.30
10.0	1.87 (±0.06)	1.08	1.23 (±0.04)	0.09	1.30 (±0.05)	0.18

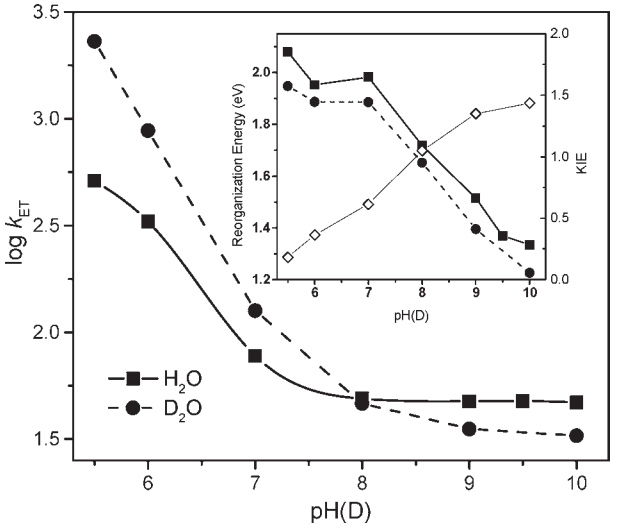

Figure 4. The pH-dependence of the rate constant of charge recombination at 10 °C in H_2O (■) and in D_2O (●). The pD values of the D_2O buffer solutions were determined by reading the pH electrode and adding 0.4. Inset: The pH-dependence of the reorganization energy on pH (■) and pD (●), and the KIE as a function of pH(D) (◊).

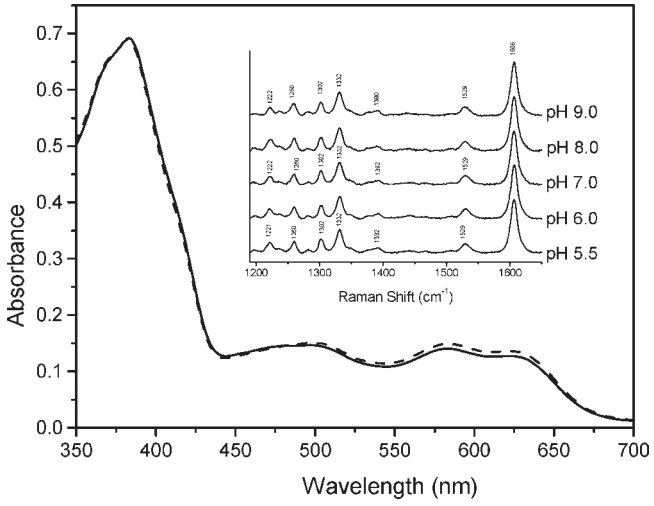

Figure 5. Absorption spectra of the $FADH^{\bullet}$ in DNA photolyase at pH 5.5 (dashed line) and pH 9.0 (solid line). Inset: Resonance Raman spectra of $FADH^{\bullet}$ in DNA photolyase at pH 5.5, 6.0, 7.0, 8.0, and 9.0.

the entropy term from the analysis for both H_2O and D_2O experiments.

Effect of Quantum Correction on Reorganization Energy and Electronic Coupling Matrix Element. The results of the analysis of the data with the semi-classical Hopfield expression including the entropy correction for the electron-transfer rate-constant with $\hbar\omega$ = 25 meV are shown in Table 3 and in Figure 3. We were unable to fit the data using $\hbar\omega$ = 200 meV, whereas a value of $\hbar\omega$ = 70 meV gave values of λ and H_{AB} that were unrealistically high (e.g., 4 eV ≤ λ ≤ 7 eV). An excellent fit to the data (indistinguishable from the classical fit) was obtained using $\hbar\omega$ = 25 meV with values of λ and H_{AB} that are slightly higher compared to those from the classical Marcus expression. The pH-dependent trends of λ and H_{AB} observed are the same as those observed with the classical Marcus expression. When $\hbar\omega$ is made even smaller (20, 15, 10, and 1 meV), the values of λ and H_{AB} approach those obtained with the classical Marcus expression. A fit with $\hbar\omega$ as a free parameter resulted in unrealistically small values (10^{-3} to 10^{-4} meV). The analysis of the data obtained in D_2O with the semi-classical Hopfield expression ($\hbar\omega$ = 25 meV) shows the same trend observed with the classical Marcus expression; λ is slightly lower in D_2O than in H_2O and decreases as a function of pD. However, the values of λ and H_{AB} in D_2O are slightly higher for the semi-classical Hopfield case compared to the classical Marcus case (Table 3).

Stability of $FADH^{\bullet}$ and $FADH^{-}$ as a Function of pH(D). For the analysis of our results, we assume that $FADH^{\bullet}$ and $FADH^{-}$

dx.doi.org/10.1021/ja2001488 |J. Am. Chem. Soc. 2011, 133, 7824–7836

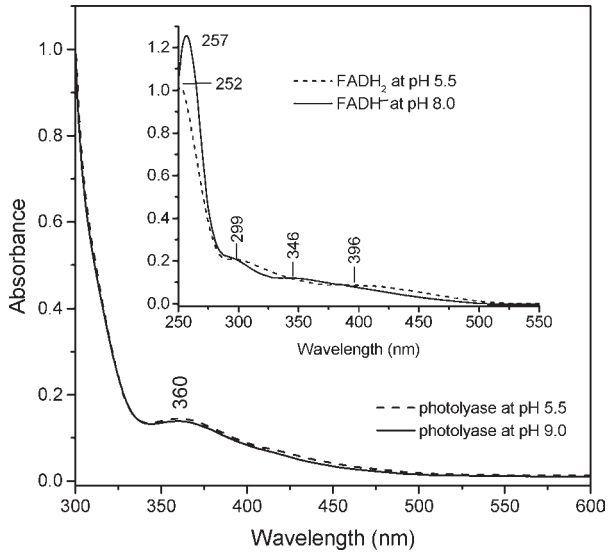

Figure 6. Absorption spectra of fully reduced FAD in photolyase without MTHF at pH 5.5 (dashed) and pH 9.0 (solid). Inset: Absorption spectra of $FADH_2$ at pH 5.5 (dashed) and $FADH^-$ at pH 8.0 (solid).

are stable over the entire pH(D) range of our study. Since the flavin hydroquinone and the flavin radical semiquinone have pK_a values around 6.7 and 8.5, respectively,[55,56] the FAD-cofactor could change protonation state within the pH(D) range of our study. Therefore, the stability of $FADH^\bullet$ and $FADH^-$ in photolyase was tested as a function of pH. Figure 5 shows absorption spectra of *E. coli* photolyase at pH 5.5 and pH 9.0; $FADH^\bullet$ is observed throughout the entire pH- and pD- (data not shown) range. We did note the presence of a small amount of oxidized FAD at higher pH values, but no evidence for the anionic radical semiquinone ($FAD^{\bullet-}$) was observed. If any $FAD^{\bullet-}$ is formed, it may rapidly decay to oxidized FAD. The resonance Raman spectra of $FADH^\bullet$ in *E. coli* photolyase in the pH range from 5.5 to 9.0 support this finding and are identical to those reported before (Figure 5, inset).[36]

The absorption spectrum of reduced FAD in solution was recorded to demonstrate the difference in absorbance between $FADH_2$ at pH 5.5 and $FADH^-$ at pH 8.0 (Figure 6, inset), in agreement with the literature.[56] The reduced FAD-cofactor in photolyase with MTHF removed by photodecomposition shows no difference in absorption at pH 5.5 and pH 9.0 (Figure 6). Since the reduced FAD is present as $FADH^-$ in photolyase at pH 7.0,[21] this result indicates that $FADH^-$ is its protonation state for the entire pH-range of this study. The absorption spectra were identical in D_2O (data not shown). Therefore, the protein environment in *E. coli* photolyase stabilizes the neutral radical semiquinone, $FADH^\bullet$, and the reduced flavin, $FADH^-$, in the same protonation state throughout the pH(D)-range from 5.5 to 10.

DISCUSSION

Our analysis shows that the reorganization energy of the charge recombination reaction between $FADH^-$ and $^{306}Trp^\bullet$ in photolyase is pH dependent. At lower pH, the reorganization energy is around 2.0 (2.3) eV, and it decreases to about 1.3 (1.5) eV at higher pH (Table 3). For the remainder of the manuscript, the values from analysis with the semi-classical Hopfield theory will be indicated between parentheses. The pH-dependence of the reorganization energy can be due to either a change in the structure of the reactants and/or the products or to a change in the mechanism of charge recombination. The pK_a values of TrpH and $TrpH^{\bullet+}$ of about 17 and 3.7, respectively,[16,47] lie outside the pH range of our study, and no change in protonation state of $^{306}TrpH$ and $^{306}Trp^\bullet$ is expected. The absorption and resonance Raman spectra show that the protonation states of $FADH^\bullet$ and $FADH^-$ in photolyase also do not change within the pH range of the study. Therefore, we rule out that changes to the structures of the reactants and products of charge recombination reaction are responsible for the pH-dependence of the reorganization energy.

To ascertain if the pH-dependence of the reorganization energy of the charge recombination is due to a change in mechanism, we tested two models by applying a global analysis fit to the data. The first model has been proposed by Byrdin et al., which explicitly includes $^{306}TrpH^{\bullet+}$ and $^{306}Trp^\bullet$ as electron acceptors (Figure 1B).[19] In this model, which we will refer to as the ET-model, charge recombination occurs from $FADH^-$ to $^{306}TrpH^{\bullet+}/^{306}Trp^\bullet$ depending on the pH and with a pK_a of 4. The pure electron transfer between $FADH^-$ and $^{306}TrpH^{\bullet+}$ is described by eq 9a and is labeled ET(I). The charge recombination between $FADH^-$ and $^{306}Trp^\bullet$ is assumed to be an ETPT mechanism in which rate-limiting electron transfer is followed by a proton transfer step. This electron transfer step is described by eq 9b and is labeled ET(II). In the second model, which we will refer to as the CEPT-model, we propose a CEPT mechanism as the higher value of the reorganization energy at low pH is consistent with such a mechanism (Figure 1C).[16] The CEPT mechanism is given by eq 9c. At higher pH values, ETPT in the form of rate-limiting electron transfer between $FADH^-$ and $^{306}Trp^\bullet$ followed by proton transfer dominates. This mechanism is the same as ET(II).

$$\mathrm{ET(I):}\quad FADH^- + {}^{306}TrpH^{\bullet+} + \rightarrow FADH^\bullet + {}^{306}TrpH \tag{9a}$$

$$\mathrm{ET(II):}\quad FADH^- + {}^{306}Trp^\bullet \rightarrow FADH^\bullet + {}^{306}Trp^- \tag{9b}$$

$$\mathrm{CEPT:}\quad FADH^- + {}^{306}Trp^\bullet + H^+ \rightarrow FADH^\bullet + {}^{306}TrpH \tag{9c}$$

Besides the difference in mechanism at lower pH (ET vs CEPT), the two models differ in the origin of the pH-dependence of the charge recombination rate constant. In the ET-model, this pH-dependence is explained by the equilibrium between $^{306}TrpH^{\bullet+}$ and $^{306}Trp^\bullet$ with a pK_a of about 4.[19] In our CEPT-model, it originates from the pH-dependence of the thermodynamic parameters that affect the CEPT rate constant.

Each model was tested with the data from the H_2O and D_2O studies in the pH(D)-range of 5.5−10. The thermodynamic parameters that were used for each model are listed in Table 4. Only the CEPT mechanism (eq 9c) explicitly requires the pH(D) and temperature dependence of the free energy change of the reaction. For both the ET(I) mechanism (eq 9a) and the ET(II) mechanism (eq 9b), the reduction potential of the tryptophan is independent of pH(D), and the temperature dependence is eliminated because no proton uptake is involved in these pure ET mechanisms; no change in the entropy is considered. H_{AB} and λ are global fit parameters for each mechanism as the reactants and products stay the same for each specific mechanism within the pH(D)-range. The fraction of charge recombination following the low pH(D) mechanism, CEPT, x, is a local fit parameter,

while $x = [1 + 10^{(pH-pK_a)}]^{-1}$ is used to describe the fraction following ET(I) in the ET-model with the pK_a as a global fit parameter.[19] All other thermodynamic parameters are determined from experimental and literature values and are kept constant with the exception of the $E_m^0(Trp^\bullet/TrpH)$ and ΔS_{uptake} pH(D)-dependent values for the CEPT mechanism. $E_m^0(TrpH^{\bullet+}/TrpH)$ = 1070 mV is used for ET(I),[47] and, by using eq 7, $E_m^0(Trp^\bullet/Trp^-)$ = 365 mV for the ET(II) mechanism with pH = 17 (the pK_a of TrpH has been estimated to be 17).[16] The rate constant of charge recombination, k_{CR}, for the ET-model and the CEPT-model at a given pH is described in the global analysis using the following two expressions:

$$\text{ET-model}: \quad k_{CR} = x \cdot k_{ET(I)} + (1 - x) \cdot k_{ET(II)} \qquad (10a)$$

$$\text{CEPT-model}: \quad k_{CR} = x \cdot k_{CEPT} + (1 - x) \cdot k_{ET(II)} \qquad (10b)$$

The results of the global analysis of the data in H_2O and D_2O solutions with both the classical Marcus expression (eq 1) and the semi-classical Hopfield expression (eq 2) for electron transfer are shown in Tables 5 and 6, and the fits to both models are shown in Figure 7. Both models fit to the data well, and the CEPT model with the semi-classical Hopfield expression gives the best overall result. For the ET-model, a pK_a of 5.8 and 5.0 is found for H_2O and D_2O, respectively, while the CEPT-model shows a transition between mechanisms (x = 0.5) around pH(D) 6.5 and 6.0 for classical Marcus and semi-classical expressions, respectively. All these values deviate from the one proposed by Byrdin et al., who used a pK_a = 4.0, the value for TrpH in solution, for the ET-model.[19]

Table 4. Thermodynamic Parameters Used for the Global Analysis Fit to the Two Models in H_2O and D_2O Solution

	$E_m^0(FADH^-/FADH^\bullet)$ (mV)	$E_m^0(Trp^\bullet/TrpH)$ (mV)	ΔS_{uptake} (eV/K)
CEPT	12.25 (45)[a]	$1070 - [pH(D) - pK_a] \cdot 53$[b]	$-R \ln(10)pH(D)$
ET(I)	12.25 (45)[a]	1070 (1070)[a]	0
ET(II)	12.25 (45)[a]	365 (395)[a]	0

[a] Values for D_2O are given between parentheses; [b] pK_a = 3.7 and 4.26 in H_2O and D_2O solutions, respectively.

For the analysis with the classical Marcus expression, the CEPT-model gives rate constants for ET(II) of 39 s^{-1} and 31 s^{-1} in H_2O and D_2O, respectively. These values are in good agreement with those predicted by Byrdin et al.; k_2 = 43 s^{-1} and 30 s^{-1} in H_2O and D_2O, respectively, for ET(II).[19] The ET-model also predicts consistent rate constants for ET(II); 44 s^{-1} and 34 s^{-1} in H_2O and D_2O, respectively. Byrdin et al. proposed a rate constant of k_1 = 40 000 s^{-1} for ET(I),[19] while both the ET-model and the CEPT-model give a much lower rate constant of 750 and 530 s^{-1} for ET(I) and CEPT, respectively, though the CEPT rate constant could reach 1500 s^{-1} at pH = 4. Finally, the value of H_{AB} for ET(I) in the ET-model is 8-times larger than the one for CEPT, and $H_{AB} = 5.2 \times 10^{-6}$ eV for CEPT is very close to a calculated value of $H_{AB} = 6.2 \times 10^{-6}$ eV for ET from ^{306}TrpH to $FADH^\bullet$ in *E. coli* photolyase.[57]

For the analysis with the semi-classical Hopfield expression for electron transfer, we used $\hbar\omega$ = 25 meV as determined above, and we find a 0.2−0.3 eV increase in λ and about a factor of 2 increase in H_{AB} as compared to the analysis with the classical Marcus expression (Tables 5 and 6). A similar trend between the values of $\hbar\omega$, λ, and H_{AB} was observed for ET between cytochrome c_2 and the *Rhodobacter sphaeroides* reaction center (RC) when classical and semi-classical analyses were compared.[58] The rate constants for ET(II) in H_2O and D_2O are slightly lower for the CEPT-model and a little higher for the ET-model for the semi-classical analysis. The value of the CEPT rate constant increases to 641 s^{-1} (1860 s^{-1} at pH 4.0), and the rate constant for ET (I) stays the same as for the analysis with the classical Marcus expression. These values are still well below the 40 000 s^{-1} that was proposed by Byrdin et al.[19] The value of H_{AB} for ET(I) is 9-times larger than for CEPT. In the latter case, the value of $H_{AB} = 10.5 \times 10^{-6}$ eV in H_2O and is still very close to the calculated value of 6.2×10^{-6} eV.[57] Comparison of our results with either the classical or semi-classical expression to earlier findings lends strong support for the CEPT-model to describe charge recombination in *E. coli* photolyase.

One significant discrepancy with the analysis of Byrdin et al. is the rate constant found at low pH, even though there is excellent

Table 5. Results of the Global Analysis Fit of the Two Models to the pH/D-Dependent Charge Recombination Rate Constants, And Calculated Charge Recombination Rate Constants and Deuterium Isotope Effects (KIE)[a]

	H_2O				D_2O				
	λ (eV)	H_{AB} (10^{-6} eV)	$\Delta G^\ddagger$ (eV)[b]	k (s^{-1})	λ (eV)	H_{AB} (10^{-6} eV)	$\Delta G^\ddagger$ (eV)[b]	k (s^{-1})	KIE
	CEPT-Model				CEPT-Model				
CEPT	2.09	5.15	[c]	[c]	1.96	7.01	[c]	[c]	[c]
	(2.31)	(10.5)			(2.12)	(11.5)			
ET(II)	1.05	0.51	0.115	39.1	1.02	0.41	0.110	31.0	1.26
	(1.25)	(1.06)	(0.162)	(37.3)	(1.19)	(0.74)	(0.149)	(30.2)	(1.23)
	ET-Model (pK_a = 5.8)				ET-Model (pK_a = 5.0)				
ET(I)	2.68	41.1	0.246	752	2.47	71.1	0.212	9520	0.08
	(2.98)	(96.5)	(0.310)	(751)	(2.72)	(145)	(0.265)	(9480)	(0.08)
ET(II)	1.53	5.89	0.226	43.6	1.60	7.32	0.243	34.0	1.28
	(1.78)	(13.3)	(0.286)	(45.4)	(1.70)	(8.36)	(0.268)	(35.6)	(1.28)

[a] Results are shown for both classical Marcus and semi-classical Hopfield electron transfer theory. Results for semi-classical expression with $\hbar\omega$ = 25 meV are given between parentheses. Rates are calculated for T = 10 °C. [b] $\Delta G^\ddagger = (\Delta G^{\circ\prime} + \lambda)^2/4\lambda$. [c] These values are pH/D-dependent for the CEPT mechanism and are listed in Table 6.

dx.doi.org/10.1021/ja2001488 |*J. Am. Chem. Soc.* 2011, 133, 7824–7836

Table 6. Results for the pH-Dependent Parameters of the Global Analysis Fit for the CEPT-Mechanism[a]

	H_2O			D_2O			
pH/D	x	$\Delta G^{\ddagger}$ (eV)[b]	k (s^{-1})	x	$\Delta G^{\ddagger}$ (eV)[b]	k (s^{-1})	KIE
5.5	1.0	0.156	533	0.80	0.130	2900	0.18
	(0.81)	(0.199)	(641)	(0.94)	(0.163)	(3220)	(0.20)
6.0	0.82	0.163	389	0.40	0.138	2150	0.18
	(0.66)	(0.208)	(470)	(0.47)	(0.171)	(2400)	(0.20)
7.0	0.26	0.179	203	0.09	0.153	1160	0.18
	(0.21)	(0.225)	(248)	(0.10)	(0.187)	(1310)	(0.19)
8.0	0.20	0.196	103	0.03	0.169	606	0.17
	(0.16)	(0.242)	(128)	(0.03)	(0.204)	(694)	(0.18)
9.0	0.45	0.213	50.7	0.02	0.185	306	0.17
	(0.33)	(0.261)	(64.0)	(0.01)	(0.221)	(359)	(0.18)
9.5	0.29	0.222	35.1	[c]	[c]	[c]	[c]
	(0.08)	(0.270)	(44.9)				
10.0	0.0	0.231	24.2	0.03	0.203	150	0.16
	(0.13)	(0.279)	(31.3)	(0.0)	(0.239)	(180)	(0.17)

[a] Results are shown for analysis with classical Marcus and the semi-classical Hopfield electron transfer theory. Results for semi-classical expression with $\hbar\omega$ = 25 meV are given between parentheses. Rates are calculated for T = 10 °C. [b] $\Delta G^{\ddagger} = (\Delta G^{\circ\prime} + \lambda)^2/4\lambda$. [c] No data recorded at pD = 9.5

agreement for the rate constant of ET(II) at high pH. They estimate k_1 = 40 000 s^{-1} for ET(I),[19] and we find 750 s^{-1} for ET(I) with pK_a = 5.8 and 1500 s^{-1} (1860 s^{-1}) for CEPT at pH 4.0. This large discrepancy is most likely due to the fact that ET(I) in the earlier work only accounts for 3% or less of the observed rate over the pH-range.[19] Thus, the rate constant k_1 = 40 000 s^{-1} is based on a very small part of the data set and represents a miniscule contribution to the observed rate at pH ≥ 5.5. Therefore, this number will have a very large uncertainty associated with it. In our analysis, CEPT (Table 6) and ET(I) contribute up to 80% and 66% to the observed rate (pH 5.5), respectively, and a much larger part of the data set is used to determine its value. In addition, we have analyzed a much larger data set including pH and temperature dependence of the rate constant, and we have used electron transfer theory with λ and H_{AB} as fit parameters and literature data to determine $\Delta G^{\circ\prime}$. Therefore, with all these restrictions, our approach results in a more accurate value of the rate constant, while the much less restricted analysis in the earlier work may easily have resulted in a significantly overestimated value. When we kept the pK_a fixed at 4 in the global analysis of the ET-model, we did find a much larger ET(I) rate constant of 15 000 s^{-1}. However, the resulting fit to the data gave a χ^2 value that is 15-times larger than any of the other fits, and this result was rejected.

Alternatively, the argument could be made that the pK_a of ^{306}TrpH in photolyase is higher than the solution value of 4 and

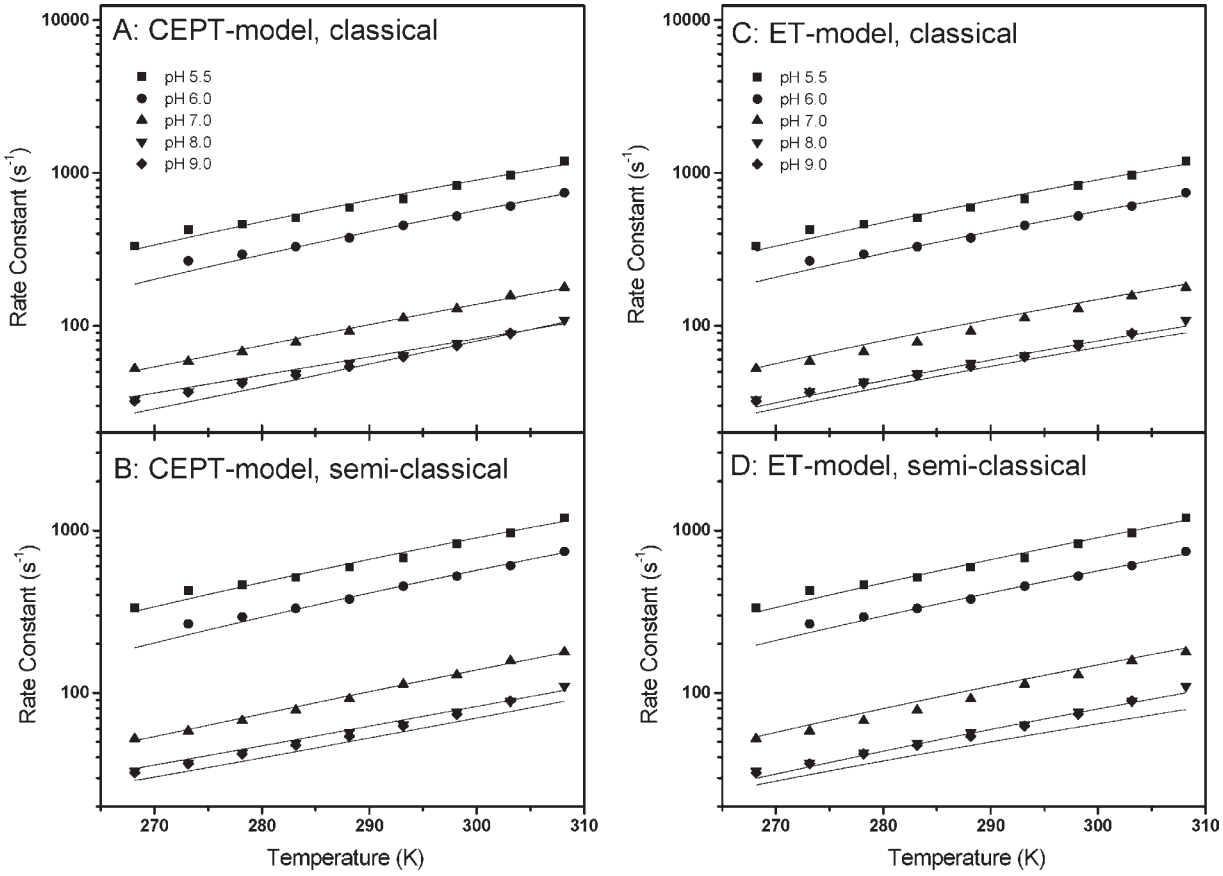

Figure 7. Results of global analysis fits of the CEPT- (A and B) and ET- (C and D) models to the pH- and temperature-dependence of the charge recombination rate constants. Either classical Marcus (A and C) or semi-classical Hopfield (B and D) electron transfer theory was used. For the analysis with the semi-classical electron transfer theory, $\hbar\omega$ was set to 25 meV. For clarity, only the data and fits (solid lines) for pH 5.5−9.0 are shown.

dx.doi.org/10.1021/ja2001488 |J. Am. Chem. Soc. 2011, 133, 7824–7836

closer to 5.8, the value obtained from the global analysis fit. Although this would explain the overestimation of k_1 in the work of Byrdin et al., it still results in unusually large values of the reorganization energy that argue against the ET-model (see below). Furthermore, ^{306}TrpH in photolyase is at the protein surface,[33] and one would expect its pK_a to be close to the solution value.

CEPT-Model versus ET-Model. Hammarström and co-workers demonstrated that the reorganization energy is an important parameter to test for a CEPT mechanism.[16] The values obtained for the reorganization energies in the ET-model are unusually high; λ = 2.7 (3.0) eV for the ET(I) mechanism. Such large reorganization energies have been observed for pure ET reactions in water or other polar solvents but not in proteins.[42,43,45,59] In proteins, pure ET reactions generally have reorganization energies between 0.7 and 1.3 eV.[43,45] Even the predicted reorganization energy of 1.5 (1.8) eV for ET(II) in the ET-model is high compared to other reported values. In addition, when the ET-model is evaluated with a fixed pK_a of 4, the solution value for TrpH which is used by Byrdin et al., or with the fraction x as a free parameter as for the CEPT-model, the reorganization energies remain high (data not shown); values of 2.7−2.8 eV and 1.2−1.3 eV are found for ET(I) and ET(II), respectively.

The reorganization energies obtained for the CEPT model are λ = 2.1 (2.3) eV and 1.1 (1.3) eV for the CEPT and ET(II) mechanisms, respectively. The value of λ for CEPT is lower than that observed for CEPT in Ru-Tyr model compounds with λ = 2.4 eV and in hydrogen-bonded phenols with λ = 1.0−2.4 eV.[16,60] Since CEPT and ET reactions in proteins have smaller solvent-contributions to the outer sphere reorganization energy, the value of λ for CEPT is expected to be lower for charge recombination in photolyase; thus, this value appears reasonable.

The reorganization energy of 1.1 (1.3) eV for the ET(II) mechanism of the CEPT model is in the expected range for pure protein electron transfer.[43,45] Pure electron transfer with either tryptophan or flavin as one of the reactants occurs with reorganization energies of 1.1−1.2 eV[61−63] and 1.0−1.4 eV,[64−68] respectively, on the basis of experiments and calculations. Higher reorganization energies of 1.8 and 2.2 eV have been measured for ET with flavin as one of the reactants and were assigned to electrostatics in the active site and to required conformational changes, respectively.[69,70] Calculations and experiments on photoinduced ET between a flavin and tryptophan predict a λ of 0.7−2.1 eV.[71,72] The values of λ larger than 1.3 eV in these studies are mainly due to solvent contributions to the outer sphere reorganization energy and, to a lesser extent, to involvement of the flavin excited state. In general, an average reorganization energy of 1.2 eV can be expected for ET involving a flavin, a tryptophan, or both. This is close to the value for the reorganization energy predicted for the ET(II) mechanism in the CEPT model.

Therefore, on the basis of the size of the reorganization energies and the discussion in the previous section, the CEPT-model, whether analyzed with the classical Marcus theory or with the semi-classical Hopfield theory, provides a much more realistic description of charge recombination in *E. coli* photolyase; thus, this model is favored over the ET-model. We stress that the global analysis fit was used as a convenient tool to evaluate two possible models for charge recombination in photolyase. Although the values of the reorganization energies appear well-defined, the values of H_{AB} and x were sensitive to variations. This was the case particularly for the ET(II) mechanism of the ET-model in D_2O experiments, for which H_{AB} and λ could vary significantly, giving rise to large, unjustifiable KIE values (∼10). This problem was not seen with the CEPT-model. It is also important to note that despite the observed variations in H_{AB} and x for the global analysis fit, the values of the reorganization energy never varied more than ±0.05 eV.

For the CEPT-model, the semi-classical Hopfield theory of the electron transfer with $\hbar\omega$ = 25 meV gave a slightly improved fit compared to the classical Marcus theory (Figure 7) along with slightly larger values of λ (increase by 0.2 eV) and H_{AB} (2-fold increase). Although a value of $\hbar\omega$ = 70 meV is more common,[73] values of 25 meV or less have been reported before, for example, in electron transfer between cytochrome c_2 and the *R. sphaeroides* photosynthetic RC in and within that RC.[58,74] The value of $\hbar\omega$ = 25 meV corresponds to a temperature of 290 K (17 °C), which falls in the middle of the temperature range of our study. Smaller values of $\hbar\omega$ resulted in minimal or no improvement in the quality of the fits, but they did bring the values of λ and H_{AB} closer to those obtained with the classical Marcus theory. This suggests that the charge recombination process in *E. coli* photolyase in the temperature range of this study is described almost equally well by the classical Marcus theory and the semi-classical Hopfield theory and that electron transfer may only be coupled to low-frequency nuclear motions. A similar conclusion was reached for electron transfer between cytochrome c_2 and the *R. sphaeroides* RC.[58]

The Deuterium Isotope Effect on Charge Recombination. The CEPT model is favored because of the large reorganization energy that is associated with the charge recombination reaction in H_2O and D_2O for pH(D) < 7.0. An important indicator of PCET is the observation of a kinetic isotope effect (KIE) for the reaction in D_2O. The ET(II) mechanism of the CEPT model predicts a small KIE of 1.26, which is consistent with our experimental data and with numbers reported for pure ET and rate-limiting ET followed by PT.[75,76] However, the expected KIE > 1 is not observed for the CEPT mechanism.[3,7,10,16,35,60,77−79] Instead, an 'inverse' KIE is observed below pH(D) 8.0; solvent isotope effects on the thermodynamic parameters may be masking the KIE that is associated with the mass of the deuteron. The 'inverse' KIE measured is the same as reported in the earlier study and has also been reported for pure electron-transfer in proteins.[19,80]

The physical and chemical properties of D_2O are well documented to be different from those of H_2O; these differences can affect the physicochemical properties of molecules that are dissolved in these solvents.[81,82] To obtain a better understanding of the observed 'inverse' KIE, we will examine each term that contributes to the rate constant. In both classical Marcus theory and semi-classical Hopfield theory, the pre-exponential factor is mainly determined by the electronic coupling matrix element, H_{AB}, while the exponential factor depends on the activation energy, $\Delta G^{\ddagger}$. Theoretical descriptions of PCET include a separate term for the proton transfer that factors in the mass of the proton.[3,4,10] Such a factor is larger in H_2O than in D_2O and does not explain the observed 'inverse' KIE. Therefore, we will focus on H_{AB} and $\Delta G^{\ddagger}$.

H_{AB} contains the strength of the electronic coupling which decays with donor−acceptor distance.[42,43] The strength of the electronic coupling depends upon the electronic/molecular orbitals that are involved in the electron transfer and the energy differences between them. Since the absorption spectrum of the FAD cofactor is the same in H_2O and D_2O solutions, the (differences between) energy levels of the FAD cofactor are not sensitive to the isotope effect. Although such data are not available for ^{306}TrpH and $^{306}Trp^{\bullet}$, we do not expect any significant change in their energy levels either. Although the solvent cavity may be slightly smaller

in D_2O, we do not expect that this has any appreciable effect on the distance between the electron donor and acceptor in photolyase. A smaller ET distance could slightly increase H_{AB} in D_2O solutions[43,45,80] but this effect is not observed for H_{AB} of the ET(II) mechanism for which the global analysis predicts $H_{AB}(D_2O) < H_{AB}(H_2O)$. Therefore, we expect the effect of D_2O on the electronic coupling matrix element to be insignificantly small with $H_{AB}(D_2O) \approx H_{AB}(H_2O)$. This is in agreement with the results from the global analysis for the CEPT-model which has $H_{AB}(D_2O) \approx 1.1$ to 1.4 times $H_{AB}(H_2O)$ (Table 5).

The activation energy, $\Delta G^{\ddagger}$, is the most likely source of the observed 'inverse' KIE and is given by:[42]

$$\Delta G^{\ddagger} = (\Delta G^{\circ\prime} + \lambda)^2/4\lambda \qquad (11)$$

Following eqs 3 and 5, it has contributions from λ, ΔS_{uptake}, $E_m^0(FADH^-/FADH^{\bullet})$, and $E_m^0(Trp^{\bullet}/TrpH)$. The reorganization energy, λ, consists of an inner sphere contribution, λ_i, and an outer sphere contribution (solvent reorganization), λ_o.[42] The reactants and products are the same in H_2O and D_2O except for the exchangeable protons; thus, λ_i is likely unchanged. From dielectric continuum theory, the outer sphere contribution is given by:[42]

$$\lambda_o = (\Delta e)^2 \left[\frac{1}{2a_1} + \frac{1}{2a_2} - \frac{1}{r}\right] \cdot \left[\frac{1}{D_{op}} - \frac{1}{D_s}\right] \qquad (12)$$

with Δe the charge that is transferred, a_1 and a_2 are the radii of the two (spherical) reactants, r is the center-to-center distance between reactants, and D_s and D_{op}, the relative dielectric constant (ε_r) and the optical dielectric constant (square of the refractive index, n) of the solvent, respectively.

At 20 °C, the values of ε_r and n are 80.21 and 1.333 and 79.89 and 1.328 for H_2O and D_2O, respectively,[83−85] to give a λ_o that is 0.7% larger in D_2O than in H_2O. A potentially smaller solvent cavity in D_2O may slightly reduce the center-to-center distance between FAD and ^{306}Trp, and the first term of λ_o could be somewhat smaller in D_2O with a_1 and a_2 assumed constant. The likely net result would be a slightly larger reorganization energy in D_2O than in H_2O. However, the global analysis finds a smaller λ in D_2O than in H_2O, with the λ in D_2O appearing to be underestimated by the global analysis fit. This result is most likely due to an underestimation of the effect of D_2O on $\Delta G^{0\prime}$.

$\Delta G^{\circ\prime}$ depends on ΔS_{uptake} and the reduction potentials of $FADH^{\bullet}$ and TrpH. The entropy term included in our analysis only takes into account the cratic (mixing) contribution of the change in entropy due to proton uptake (ΔS_{uptake}), which is the same in H_2O and D_2O solutions for properly adjusted pH and pD values (eq 4b). The much smaller unitary contribution (solute−solvent interactions) to ΔS_{uptake} is not considered. Since hydrogen bonding interactions are thought to increase by 10% in D_2O, the unitary term may be up to 10% larger in D_2O.[86,87] This would cause ΔS_{uptake} to be slightly smaller (less negative) in D_2O than in H_2O and would give rise to a small *increase* in both $\Delta G^{\circ\prime}$ and $\Delta G^{\ddagger}$, and, therefore, to a small *decrease* in k_{CEPT} in D_2O. The increase of $E_m^0(FADH^-/FADH^{\bullet})$ in photolyase by 45 ± 6 mV in D_2O solutions also leads to an *increase* in $\Delta G^{\ddagger}$ and a *decrease* of k_{CEPT} in D_2O. Therefore, the solvent isotope effects on ΔS_{uptake} and $E_m^0(FADH^-/FADH^{\bullet})$ cannot explain the observed 'inverse' KIE.

Finally, we consider the effect of D_2O on $E_m^0(Trp^{\bullet}/TrpH)$. In our analysis, we have taken into account the fact that the pK_a of a weak acid increases between 0.4 and 0.8 in D_2O,[50−52] and the pK_a of $^{306}TrpH^{\bullet+}$ has been proposed to increase by 0.56 in D_2O.[19] Such an increase introduces a 'horizontal' shift in the pH(D)-dependence of $E_m^0(Trp^{\bullet}/TrpH)$ in D_2O (eq 8) and causes an increase in $E_m^0(Trp^{\bullet}/TrpH)$ of about 30 mV at pD values above its pK_a^D. This would results in a more negative $\Delta G^{\circ\prime}$ and in a decrease in $\Delta G^{\ddagger}$ which, in turn, leads to an *increase* in k_{CEPT}. The effect is canceled out by the +45 mV increase measured in $E_m^0(FADH^-/FADH^{\bullet})$. Therefore, $E_m^0(Trp^{\bullet}/TrpH)$ must increase by more than 45 mV to cause a more negative $\Delta G^{\circ\prime}$, and a decrease in $\Delta G^{\ddagger}$ that would explain the increase in k_{CEPT} in D_2O. Either the pK_a of $^{306}TrpH^{\bullet+}$ increases by more than 0.56 in D_2O or $E_m^0(Trp^{\bullet}/TrpH)$ is at least 45 mV more positive in D_2O. If some combination of these changes occur, it would result in a more negative $\Delta G^{\circ\prime}$, a *decrease* in $\Delta G^{\ddagger}$, and an *increase* in k_{CEPT} in D_2O.

Although we cannot rule out that small, seemingly insignificant changes to H_{AB}, λ, and ΔS_{uptake} in D_2O may add up to a more substantial solvent isotope effect, the most likely cause of the 'inverse' KIE is an increase in $E_m^0(Trp^{\bullet}/TrpH)$ in D_2O. This conclusion is not merely a product of the global analysis, because global analysis of the CEPT-model does properly predict the observed KIE of ET(II). An increase in $E_m^0(Trp^{\bullet}/TrpH)$ or a larger ΔpK_a of $TrpH^{\bullet+}$ in D_2O would decrease the activation energy and increase the rate constant of the CEPT. On the basis of theoretical considerations and experimental observations, a KIE of 1 to 2 is expected for CEPT that involves short-range, adiabatic proton transfer.[3,7,35,60,77,88−90] Our analysis indicates that it is possible that such a small but real KIE is masked by a solvent isotope effect on the thermodynamic parameters of the ET cofactors, resulting in the observed inverse KIE of 0.18. Therefore, the observed 'inverse' KIE of the CEPT-mechanism can be explained by the solvent isotope effect on mainly the reduction potentials of the donor and acceptor molecules, while other factors (λ, H_{AB}, and ΔS_{uptake}) may make minor contributions. This further supports the presence of a CEPT mechanism at low pH during charge recombination in *E. coli* photolyase.

Switching between CEPT and ET in Photolyase. The following analysis is the same whether the classical Marcus theory or the semi-classical Hopfield theory of electron transfer is used. Although H_{AB} for the CEPT mechanism is constant over the pH-range, the rate constant of charge recombination for this mechanism varies with pH because of the pH-dependence of $E_m^0(Trp^{\bullet}/TrpH)$ and the entropy correction for the proton uptake. The rate constant at 10 °C varies from 530 (640) s^{-1} at pH 5.5 to 24 (31) s^{-1} at pH 10 (Table 6). The pH-dependence of the CEPT rate constant has the interesting consequence in that it becomes smaller than the pH-independent rate constant of ET(II) at pH 9.5. Although the pH-dependence of fraction x (Table 6) indicates that the ET(II) mechanism becomes dominant above pH 6.5, the global analysis of the CEPT model suggests that the CEPT mechanism still contributes at higher pH values. This may be due to the limited temperature range of the experiments at higher pH values in H_2O experiments. The $FADH^{\bullet}$ state of the enzyme was much more stable in D_2O experiments, and a larger temperature range could be studied. At higher pD values, the global analysis of these data shows a much smaller contribution of CEPT. Since our analysis shows that $k_{CEPT} \approx k_{ET(II)}$ around pH 9.5 and that the switch between CEPT and ET(II) occurs between pH 6 and pH 7, it is not likely that the CEPT and ET(II) mechanisms compete on a kinetic basis. Either a real switch occurs on the basis of favorable thermodynamics for one mechanism or the availability of a suitable proton donor with a pK_a around 6.5 modulates the two mechanisms.

Analysis of the thermodynamic and other parameters of the CEPT and ET(II) mechanisms provides insight into the switch between the two mechanisms around pH 7. The driving force, $\Delta G^{\circ\prime}$, of the CEPT mechanism becomes less negative with increasing pH but is more favorable than $\Delta G^{\circ\prime}$ of the ET(II) mechanism which is unchanged over the pH range (Tables 5 and 6). The activation energy, $\Delta G^{\ddagger}$, of the CEPT mechanism increases with pH and is larger than that of the ET(II) mechanism over the entire pH range. The apparent switch between CEPT and ET occurs below pH 7. In that pH range, $\Delta G^{\circ\prime}$ is about 8 times larger for CEPT than for ET, and $\Delta G^{\ddagger}$ is larger for CEPT than for ET. This suggests that a delicate balance between a favorable driving force and an unfavorable activation energy may determine the switch between CEPT and ET mechanisms, similar to what has been proposed for the model compounds studied by Hammarström and co-workers.[15,16] Unlike the model compounds, no normal KIE is observed, and the CEPT rate constant is larger than the ET(PT) rate constant in photolyase.

The 'inverse' KIE is most likely due to modification of the thermodynamic parameters in D_2O solutions, especially, $E_m^0(Trp^{\bullet}/TrpH)$ as discussed above. Since the observed 'inverse' KIE of the CEPT mechanism indicates that there may only be a small isotope effect (KIE $\approx 1-1.5$) due to the difference in mass, there is likely only a low-barrier adiabatic proton-transfer over a short distance, and the proton donor may be hydrogen-bonded to $^{306}Trp^{\bullet}$.[7,35,60,77,88−91] This suggests that a balance between $\Delta G^{\circ\prime}$ and $\Delta G^{\ddagger}$ may not be the only contribution to the switch and that the availability of the proton must also be considered. The crystal structure shows that there are no amino acids sufficiently close to ^{306}TrpH to act as proton-donor during CEPT but a water molecule with its oxygen atom at 2.8 Å from the ^{306}TrpH indole nitrogen could fulfill that role.[33] The presence of a water molecule hydrogen bonded to $^{306}Trp^{\bullet}$ could be tested as a function of pH by using resonance Raman spectroscopy. Resonance Raman spectra of $^{306}Trp^{\bullet}$ in photolyase at pH(D) 7.4 show no evidence of a hydrogen bond to the indole nitrogen,[92] in agreement with a switch to the ET(II) mechanism at that pH.

The global analysis predicts that H_{AB} is about 10 times larger for CEPT than for ET(II). Since the FAD cofactor is the same in the reactant and product states for both mechanisms, this difference would be due to tryptophan in the product state. In this state, tryptophan is TrpH and Trp^- for the CEPT and ET mechanism, respectively. This would suggest that the presence of Trp^- results in poorer electronic coupling between reactant and product states assuming the distance between the FAD cofactor and ^{306}TrpH does not change with pH.

Finally, $-\Delta G^{\circ\prime}$ is significantly smaller than the reorganization energy for either mechanism. This indicates that either mechanism occurs in the Marcus normal region and will display a temperature dependent rate constant.[42] A small temperature dependence of the rate constant is already observed within the temperature range of our study, and extension of our study to lower temperatures could uncover additional details about either mechanism.

CONCLUSIONS

The charge recombination between $FADH^-$ and $^{306}Trp^{\bullet}$ in *E. coli* photolyase is characterized by a pH-dependent reorganization energy. Global analysis of the data shows that this pH-dependence is best explained by a model that predicts that charge recombination occurs through concerted electron proton transfer (CEPT) with a large reorganization energy ($\lambda = 2.1-2.3$ eV) below pH 7 and through rate-limiting electron transfer followed by proton transfer (ETPT) with a lower reorganization energy ($\lambda = 1.1-1.3$ eV). The switch from the CEPT to the ET mechanism occurs at a pH of about 6.5 and is not due to a straightforward kinetic competition on the basis of the rate constants. It is most likely due to either a delicate balance between driving force ($\Delta G^{\circ\prime}$) and activation energy ($\Delta G^{\ddagger}$) or the availability of a nearby proton donor. As judged from the quality of the global analysis fit, the semi-classical Hopfield theory of electron transfer provides a slightly better analysis of our results than the classical Marcus theory.

The charge recombination displays an unexpected 'inverse' isotope effect below pH 8 for the proposed CEPT mechanism. Our analysis indicated that a small, normal KIE of about 1.4 can easily be masked by solvent isotope effects on $E_m^0(FADH^-/FADH^{\bullet})$ and $E_m^0(Trp^{\bullet}/TrpH)$ that lower $\Delta G^{\ddagger}$ and increase k_{CEPT} in D_2O solutions. Since $E_m^0(FADH^-/FADH^{\bullet})$ in photolyase increases by 45 ± 6 mV in D_2O solutions, we predict that $E_m^0(Trp^{\bullet}/TrpH)$ increases by at least that amount. The $E_m^0(Trp^{\bullet}/TrpH)$ itself may increase in D_2O or can appear to increase as a result of an increase in the pK_a of $TrpH^{\bullet+}$.

AUTHOR INFORMATION

Corresponding Author
schelvisj@mail.montclair.edu

ACKNOWLEDGMENT

This research is supported by a grant from NSF to J.P.M.S. (MCB-0920013). Y.M.G. and C.R. acknowledge support from the Lafayette College Academic Research Committee and the Chemistry Department.

REFERENCES

(1) Reece, S. Y.; Hodgkiss, J. M.; Stubbe, J.; Nocera, D. G. *Philos. Trans. R. Soc., B* **2006**, *361*, 1351–1364.
(2) Stubbe, J.; Nocera, D. G.; Yee, C. S.; Chang, M. C. Y. *Chem. Rev.* **2003**, *103*, 2167–2201.
(3) Cukier, R. I.; Nocera, D. G. *Annu. Rev. Phys. Chem.* **1998**, *49*, 337–369.
(4) Hammes-Schiffer, S. *Acc. Chem. Res.* **2001**, *34*, 273–281.
(5) Mayer, J. M. *Annu. Rev. Phys. Chem.* **2004**, *55*, 363–390.
(6) Georgievskii, Y.; Stuchebrukhov, A. A. *J. Chem. Phys.* **2000**, *113*, 10438–10450.
(7) Cukier, R. I. *J. Phys. Chem. B* **2002**, *106*, 1746–1757.
(8) Costentin, C. *Chem. Rev.* **2008**, *108*, 2145–2179.
(9) Hammes-Schiffer, S.; Soudackov, A. V. *J. Phys. Chem. B* **2008**, *112*, 14108–14123.
(10) Kuznetsov, A. M.; Ulstrup, J. *J. Phys. Org. Chem.* **2010**, *23*, 647–659.
(11) Stubbe, J.; van der Donk, W. A. *Chem. Rev.* **1998**, *98*, 705–762.
(12) Giese, B.; Wang, M.; Gao, J.; Stolz, M.; Müller, P.; Graber, M. *J. Org. Chem.* **2009**, *74*, 3621–3625.
(13) Shih, C.; Museth, A. K.; Abrahamsson, M.; Blanco-Rodriguez, A. M.; Di Bilio, A. J.; Sudhamsu, J.; Crane, B. R.; Ronayne, K. L.; Towrie, M.; Vlček, A., Jr.; Richards, J. H.; Winkler, J. R.; Gray, H. B. *Science* **2008**, *230*, 1760–1762.
(14) Sjödin, M.; Styring, S.; Åkermark, B.; Sun, L.; Hammarström, L. *J. Am. Chem. Soc.* **2000**, *122*, 3932–3936.
(15) Sjödin, M.; Ghanem, R.; Polivka, T.; Pan, J.; Styring, S.; Sun, L.; Sundström, V.; Hammarström, L. *Phys. Chem. Chem. Phys.* **2004**, *6*, 4851–4858.
(16) Sjödin, M.; Styring, S.; Wolpher, H.; Xu, Y.; Sun, L.; Hammarström, L. *J. Am. Chem. Soc.* **2005**, *127*, 3855–3863.

(17) Aubert, C.; Vos, M. H.; Mathis, P.; Eker, A. P. M.; Brettel, K. *Nature* **2000**, *405*, 586–590.
(18) Kapetanaki, S. M.; Ramsey, M.; Gindt, Y. M.; Schelvis, J. P. M. *J. Am. Chem. Soc.* **2004**, *126*, 6214–6215.
(19) Byrdin, M.; Sartor, V.; Eker, A. P. M.; Vos, M. H.; Aubert, C.; Brettel, K.; Mathis, P. *Biochim. Biophys. Acta* **2004**, *1655*, 64–70.
(20) Sancar, A. *Chem. Rev.* **2003**, *103*, 2203–2237.
(21) Kim, S.-T.; Sancar, A.; Essenmacher, C.; Babcock, G. T. *Proc. Natl. Acad. Sci. U.S.A.* **1993**, *90*, 8023–8027.
(22) Jorns, M. S.; Sancar, G. B.; Sancar, A. *Biochemistry* **1984**, *23*, 2673–2679.
(23) Gindt, Y. M.; Vollenbroek, E.; Westphal, K.; Sackett, H.; Sancar, A.; Babcock, G. T. *Biochemistry* **1999**, *38*, 3857–3866.
(24) Heelis, P. F.; Sancar, A. *Biochemistry* **1986**, *25*, 8163–8166.
(25) Byrdin, M.; Eker, A. P. M.; Vos, M. H.; Brettel, K. *Proc. Natl. Acad. Sci. U.S.A.* **2003**, *100*, 8676–8681.
(26) Saxena, C.; Sancar, A.; Zhong, D. *J. Phys. Chem. B* **2004**, *108*, 18026–18033.
(27) Partch, C. L.; Sancar, A. *Photochem. Photobiol.* **2005**, *81*, 1291–1304.
(28) Lin, C.; Shalitin, D. *Annu. Rev. Plant Physiol. Plant Mol. Biol.* **2003**, *54*, 469–496.
(29) Zeugner, A.; Byrdin, M.; Bouly, J. P.; Bakrim, N.; Giovani, B.; Brettel, K.; Ahmad, M. *J. Biol. Chem.* **2005**, *280*, 19437–19440.
(30) Brettel, K.; Byrdin, M. *Curr. Opin. Struct. Biol.* **2010**, *20*, 693–701.
(31) Byrdin, M.; Lukacs, A.; Thiagarajan, V.; Eker, A.P.M.; Brettel, K.; Vos, M.H. *J. Phys. Chem. A* **2010**, *114*, 3207–3214.
(32) Li, Y. F.; Heelis, P. F.; Sancar, A. *Biochemistry* **1991**, *30*, 6322–6329.
(33) Park, H.-W.; Kim, S.-T.; Sancar, A.; Deisenhofer, J. *Science* **1995**, *268*, 1866–1872.
(34) Heelis, P. F.; Payne, G.; Sancar, A. *Biochemistry* **1987**, *26*, 4634–4640.
(35) Jenson, D. L.; Evans, A.; Barry, B. A. *J. Phys. Chem. B* **2007**, *111*, 12599–12604.
(36) Schelvis, J. P. M.; Ramsey, M.; Sokolova, O.; Tavares, C.; Cecala, C.; Connell, K.; Wagner, S.; Gindt, Y. M. *J. Phys. Chem. B* **2003**, *107*, 12352–12362.
(37) Wang, B.; Jorns, M. S. *Biochemistry* **1989**, *28*, 1148–1152.
(38) Glasoe, P. K.; Long, F. A. *J. Phys. Chem.* **1960**, *64*, 188–190.
(39) Covington, A. K.; Paabo, M.; Robinson, R. A.; Bates, R. G. *Anal. Chem.* **1968**, *40*, 700–706.
(40) Sokolowsky, K.; Newton, M.; Lucero, C.; Wertheim, B.; Freedman, J.; Cortazar, F.; Czochor, J.; Schelvis, J. P. M.; Gindt, Y. M. *J. Phys. Chem. B* **2010**, *114*, 7121–7130.
(41) Gindt, Y. M.; Schelvis, J. P. M.; Thoren, K. L.; Huang, T. H. *J. Am. Chem. Soc.* **2005**, *127*, 10472–10473.
(42) Marcus, R. A.; Sutin, N. *Biochim. Biophys. Acta* **1985**, *811*, 265–322.
(43) Gray, H. B.; Winkler, J. R. *Q. Rev. Biophys.* **2003**, *36*, 341–372.
(44) Hopfield, J. J. *Proc. Natl. Acad. Sci. U.S.A.* **1974**, *71*, 3640–3644.
(45) Moser, C. C.; Dutton, P. L. In *Protein Electron Transfer*; Bendall, D. S., Ed.; BIOS Scientific Publishers: Oxford, 1996; Chapter 1.
(46) Harriman, A. *J. Phys. Chem.* **1987**, *91*, 6102–6104.
(47) Tommos, C.; Skalicky, J. J.; Pilloud, D. L.; Wand, A. J.; Dutton, P. L. *Biochemistry* **1999**, *38*, 9495–9507.
(48) Hille, R. *Biochemistry* **1991**, *30*, 8522–8529.
(49) Hirst, J.; Ackrell, A. C.; Armstrong, F. A. *J. Am. Chem. Soc.* **1997**, *19*, 7434–7439.
(50) McDougall, A. O.; Long, F. A. *J. Phys. Chem.* **1962**, *66*, 429–433.
(51) Paabo, M.; Bates, R. G. *J. Phys. Chem.* **1969**, *73*, 3014–3017.
(52) Robinson, R. A.; Paabo, M.; Bates, R. G. *J. Res. Nalt. Bur. Stand., Sect. A* **1969**, *73*, 299–308.
(53) Su., Q.; Klinman, J. P. *Biochemistry* **1999**, *38*, 8572–8581.
(54) Hays, A.-M. A.; Vassiliev, I. R.; Golbeck, J. H.; Debus, R. J. *Biochemistry* **1999**, *38*, 11851–11865.
(55) McFarland, J. T. In *Biological Applications of Raman Spectroscopy*, Vol. 2; Spiro, T. G., Ed.; Wiley and Sons: New York, 1987; pp 211−303.
(56) Massey, V.; Hemmerich, P. *Biochem. Soc. Trans.* **1980**, *8*, 246–257.
(57) Cheung, M. S.; Daizadeh, I.; Stuchebrukhov, A. A.; Heelis, P. F. *Biophys. J.* **1999**, *76*, 1241–1249.
(58) Venturoli, G.; Drepper, F.; Williams, J. C.; Allen, J. P.; Lin, X.; Mathis, P. *Biophys. J.* **1998**, *74*, 3226–3240.
(59) Page, C. C.; Moser, C.C.; Chen, X.; Dutton, P. L. *Nature* **1999**, *402*, 47–52.
(60) Rhile, I. J.; Markle, T. F.; Nagao, H.; DiPasquale, A. G.; Lam, O. P.; Lockwood, M. A.; Rotter, K.; Mayer, J. M. *J. Am. Chem. Soc.* **2006**, *128*, 6075-6088. 101.
(61) Lee, E.; Medvedev, E. S.; Stuchebrukhov, A. A. *J. Chem. Phys.* **2000**, *112*, 9015–9024.
(62) Aoudia, M.; Guliaev, A. B.; Leontis, N. B.; Rodgers, M. A. *J. Biophys. Chem.* **2000**, *83*, 121–140.
(63) Tang, J.; Li, X.-Y.; Fu, K.-X.; Liu, J.-F.; Lu, S.-Z. *Chem. Phys.* **2005**, *312*, 21–29.
(64) Capeillere-Blandin, C. *Biochimie* **1995**, *77*, 516–530.
(65) Wilson, E. K.; Huang, L.; Sutcliffe, M. J.; Mathews, F. S.; Hille, R.; Scrutton, N. S. *Biochemistry* **1997**, *36*, 41–48.
(66) Twitchett, M. B.; Ferrer, J. C.; Siddarth, P.; Mauk, A. G. *J. Am. Chem. Soc.* **1997**, *119*, 435–436.
(67) Andersen, N. H.; Hervás, M.; Navarro, J. A.; De la Rosa, M.; Ulstrup, J. *Inorg. Chim. Acta* **1998**, *272*, 109–114.
(68) Roth, J. P.; Wincek, R.; Nodet, G.; Edmondson, D. E.; McIntire, W. S.; Klinman, J. P. *J. Am. Chem. Soc.* **2004**, *126*, 15120–15131.
(69) Roth, J. P.; Klinman, J. P. *Proc. Natl. Acad. Sci. U.S.A.* **2003**, *100*, 62–67.
(70) Falzon, L.; Davidson, V. L. *Biochemistry* **1996**, *35*, 12111–12118.
(71) Callis, P. R.; Liu, T. *Chem. Phys.* **2006**, *326*, 230–239.
(72) Crovetto, L.; Braslavsky, S. E. *J. Phys. Chem. A* **2006**, *110*, 7307–7315.
(73) Moser, C. C.; Keske, J. M.; Warncke, K.; Farid, R. S.; Dutton, P. L. *Nature* **1992**, *355*, 796–802.
(74) Wang, H.; Lin, S.; Katilius, E.; Laser, C.; Allen, J. P.; Williams, J. C.; Woodbury, N. *J. Phys. Chem. B* **2009**, *113*, 818–824.
(75) Bishop, G. R.; Davidson, V. L. *Biochemistry* **1998**, *37*, 11026–11032.
(76) Soriano, G. M.; Cramer, W. A. *Biochemistry* **2001**, *40*, 15109–15116.
(77) Karge, M.; Irrgang, K.-D.; Renger, G. *Biochemistry* **1997**, *36*, 8904–8913.
(78) Decornez, H.; Hammes-Schiffer, S. *J. Phys. Chem. A* **2000**, *104*, 9370–9384.
(79) Edwards, S. J.; Soudackov, A. V.; Hammes-Schiffer, S. *J. Phys. Chem. A* **2009**, *113*, 2117–2126.
(80) Farver, O.; Zhang, J.; Chi, Q.; Pecht, I.; Ulstrup, J. *Proc. Natl. Acad. Sci. U.S.A.* **2001**, *98*, 4426–4430.
(81) Lopez, M. M.; Makhatadze, G. I. *Biophys. Chem.* **1998**, *74*, 117–125.
(82) Schowen, K. B.; Schowen, R. L. *Meth. Enzym* **1982**, *87*, 551–606.
(83) Vidulich, G. A.; Evans, D. F.; Kay, R. L. *J. Phys. Chem.* **1967**, *71*, 656–662.
(84) Daimon, M.; Masumura, A. *Appl. Opt.* **2007**, *46*, 3811–3820.
(85) Nikogosyan, D. N. In *Properties of Optical and Laser-Related Materials: A Handbook*; Wiley and Sons: Chichester, England, 1997.
(86) Marcus, Y.; Ben-Naim, A. *J. Chem. Phys.* **1985**, *83*, 4744–4759.
(87) Katsir, Y.; Shapira, Y.; Mastai, Y.; Dimova, R.; Ben-Jacob, E. *J. Phys. Chem. B* **2010**, *114*, 5755–5763.
(88) Turro, C.; Chang, C. K.; Leroi, G. E.; Cukier, R. I.; Nocera, D. G. *J. Am. Chem. Soc.* **1992**, *114*, 4013–15.
(89) Roberts, J. A.; Kirby, J. P.; Nocera, D. G. *J. Am. Chem. Soc.* **1995**, *117*, 8051–8052.
(90) Levich, V. G.; Dogonadze, R. R.; German, E. D.; Kuznetsov, A. M.; Kharkats, Y. I. *Electrochim. Acta* **1970**, *15*, 353–367.
(91) Krishtalik, L. I. *Biochim. Biophys. Acta* **2000**, *1458*, 6–27.
(92) Gurudas, U.; Schelvis, J. P. M. *J. Am. Chem. Soc.* **2004**, *126*, 12788–12789.